Stress analysis for concrete materials under multiple freeze-thaw cycles

Fuyuan Gong, Evdon Sicat, Dawei Zhang, Tamon Ueda

Journal of Advanced Concrete Technology, volume 13 (2015), pp. 124-134

Scientific paper

Stress Analysis for Concrete Materials under Multiple Freeze-Thaw Cycles

Fuyuan Gong[1], Evdon Sicat[2], Dawei Zhang[3*] and Tamon Ueda[4]

Received 21 August 2014, accepted 25 February 2015 doi:10.3151/jact.13.124

Abstract

Once ice forms in highly saturated concrete material, internal tensile stress will be generated and causes damage to the material, which is a serious problem for concrete structures in cold and wet regions. On one hand, each component (porous body, ice and liquid) should satisfy the compatibility of stress and strain, which has been discussed by the poromechanical theories. On the other hand, if some empty voids exist, the hydraulic pressure will release when liquid water escapes from the expanded area according to Darcy's law. Recent closed freeze-thaw tests on the saturated mortar showed a consistent tendency: as the number of freeze-thaw cycles (FTC) increases, the deformation changes from the expansion to the contraction. In order to make clear the physical and mechanical changes during this process, a more comprehensive hydraulic model is developed, which combines both the mechanisms mentioned above. The estimated strain behavior by this model is in a good agreement with experimental measurements, and also, it has good potential and is more flexible to be applied to different cases such as different saturation degrees and cooling rates. The permeability change can be also considered in this model as a reflection of frost damage level.

1. Introduction

Frost damage is an important issue for concrete structures, and has been studied for several decades. The deformation behavior and degradation of properties by frost action has been well studied at the material level. Kaufmann (2002) developed a qualitative sequential damage model, separating a freeze-thaw cycle into five phases and discussed in detail. Fagerlund (2002) discussed the different effects between open and closed freeze-thaw tests (FTC test with open or closed moisture condition), and the effect of saturation degree. For the open test, the deformation measure by Hasan *et al*. (2004) up to 300 cycles showed a continually increasing behavior. This agrees with our common sense and can be explained easily by the existing models. However, recent closed tests up to 30 cycles by the authors showed different phenomenon: there was expansion during first few cycles, but converted to contraction as the number of cycle increased (Sicat *et al*, 2013). Although the damage of material would affect the measured deformation, this change of tendency can only be explained by the change of forces: from positive forces dominant to negative forces dominant. Thus, more comprehensive stress model is needed to explain this complex strain behavior. The stress that causes frost damage is believed as the hydraulic pressure at the beginning. Powers (1949) developed the hydraulic pressure model based on Darcy's law, and according to that model, the maximum spacing factor of the entrained air can be determined so that the damage can be avoided. Recent studies discussed that, other than hydraulic pressure, the crystallization pressure is another mechanism (Scherer, 2005), because damage was observed even in partially saturated cases, in which the hydraulic pressure can be avoided. In addition, due to the thermodynamic equilibrium between three phases of moisture, there is always a cryosuction pressure in the unfrozen water. Sun and Scherer (2010a) also developed the mathematical way to calculate the overall stress and strain caused by crystallization and cryosuction pressures. Coussy and Monteiro's model (2008) was developed based on the poromechanics and was improved later (2009), which included hydraulic pressure and cryosuction. However, both Sun's and Coussy's models ignore the hydraulic flow and pressure release like Powers' model. Once the specimen is sealed, the internal forces are thought to be almost the same during each cycle. It is true for a few cycles because the permeability of cementitious materials is very small. But as the number of cycle increases, damage will accumulate and the liquid water can move more easily. Therefore, the pressure release should also be considered in this problem.

In this paper, we will combine all the mechanisms mentioned above to obtain a more comprehensive, flexible but not too complex model to explain the measured strain behavior under closed FTC test. Crystallization pressure and cryosuction pressure are static pressures that only rely on the temperature and pore size distribution, while the hydraulic pressure is a dynamic

[1]Graduate Student, Lab of Engineering for Maintenance System, Graduate School of Engineering, Hokkaido University, Sapporo, Japan.
[2]Engineer, Sumitomo Mitsui Construction, Tokyo, Japan
[3]Associate Professor, College of Civil Engineering and Architecture, Zhejiang University, China.
*Corresponding author, *E-mail*: dwzhang@zju.edu.cn
[4]Professor, Lab of Engineering for Maintenance System, Faculty of Engineering, Hokkaido University, Japan.

pressure which depends on the permeability of the material. Previous studies have shown that there is no significant change in pore size distribution during the first few FTCs (Sun, 2010b), so it means the crystallization pressure and cryosuction pressure are not responsible to this tendency change (expansion at the beginning but converted to contraction at last), and the main reason is the hydraulic pressure reduction due to the permeability increment caused by frost damage accumulation (Yang *et al*, 2006). The measured deformation in different cycles is used to verify the proposed model. And the application potential of this model is also discussed at last.

2. Theoretical model

2.1 Existing hydraulic pressure models

There are two main hydraulic theories for the freezing process in porous material. One is proposed by Powers (1949), aiming at discussing the suitable spacing factor of the air bubbles to avoid frost damage in the air-entrained concrete. In his model, it was assumed that all the liquid water can be expelled into the entrained air once ice forms in the surrounding material. According to Darcy's law, a pressure gradient is necessary to drive such kind of water flow, thus hydraulic pressure is generated.

Figure 1 shows the basic concept of Powers' model. The central circle represents the empty air void with a radius of *r*, and the influential volume has a radius of *R*. Since the deformation of porous body was neglected, the expanded volume during ice formation should be balanced by the flow into the air void. According to this assumption and Darcy's law, Powers gave the hydraulic pressure at x ($r \le x \le R$) along the radial direction as:

$$p_h(x) = \frac{\eta}{k} \cdot \frac{1}{3}(1.09 - 1/S_r) \cdot \phi \cdot \frac{dw_f}{dT}\frac{dT}{dt} \cdot \int_r^R \left(\frac{R^2}{x^2} - x \right) dx \quad (1)$$

where $p_h(x)$ is the hydraulic pressure at each location, k is the permeability of porous material (m^2), η is the viscosity of liquid water ($Pa \cdot s$), S_r is the saturation degree, ϕ is the void ratio, dw_f/dT is the ice forming rate as temperature changes, which depends on the pore size distribution, and finally dT/dt is the cooling rate.

Other than Powers' model, Coussy and Monteiro (2009) ignored the water flow, and proposed a poromechanical model for saturated porous materials, in which the increased volume can be balanced by the self-compression of liquid and solid water, and the pore pressure p_h is approximately obtained as follows (Coussy and Monteiro, 2009):

$$p_h \approx 0.09 \cdot \frac{\psi_C}{\psi_C / K_C + (1-\psi_C)/K_L} \quad (2)$$

where ψ_C is the ice content, $1-\psi_C$ 1 is the liquid water content. K_C and K_L are the bulk moduli of the ice and liquid, respectively. This model also describes an ideal condition based on the assumption that the hydraulic pressure resulting from the volume change cannot be released (like in the sealed condition or the case of air voids that are very far apart from each other). So actually this model shows the upper bound that the pore pressure could reach.

However, in reality, both water flow and self-compression exist, and which would be the dominant effect depends on the distribution of empty pores (like entrained or entrapped air) and permeability of the materials. That is, an upper bound of hydraulic pressure will be reached if there is only self-compression effect. But if the liquid water can move more easily to the empty voids (when empty voids are closer to each other or the permeability becomes bigger), the hydraulic pressure will release due to the escaped flow. Then if the water flow becomes the dominant effect, the hydraulic pressure will decrease and even become negligible. For example, **Fig. 2** shows the measured deformation on the water-saturated mortar with closed moisture condition

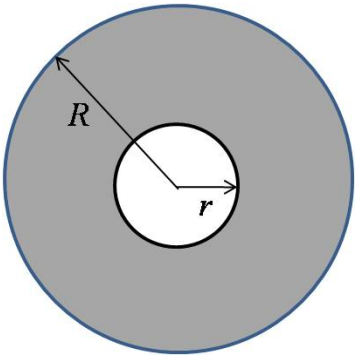

Fig. 1 Empty space and influential volume.

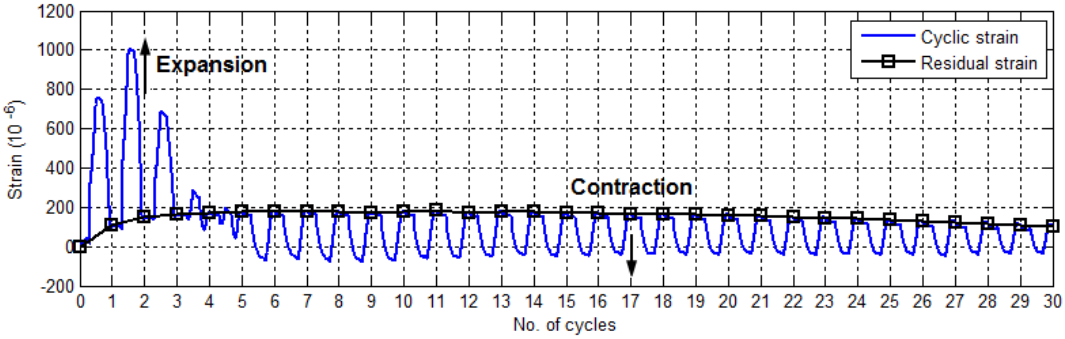

Fig. 2 Strain behavior during 30 cycles (water saturated, sealed and without thermal strain) (Sicat *et al*, 2013).

during 30 freeze-thaw cycles (Sicat *et al*. 2013). The reversing strain behavior from expansion at the beginning to contraction at last also reflects the change of total internal pore pressure: from positive value to negative value. The total pore pressure is the sum of hydraulic, crystallization and cryosuction pressures, and the crystallization and cryosuction pressures are always coexisting and regarded unchanged during the test (details will be discussed later). The sum of crystallization and cryosuction pressure is negative under the given environmental condition, but the hydraulic pressure is large enough at the beginning so that the total pressure is still positive. Since this total internal pressure can easily exceed the tensile strength of the porous body, damage will happens as internal micro-cracks and the permeability will increase (Yang *et al*. 2006). Then the hydraulic pressure will decrease until it cannot cause further damage, and the total internal pressure will become negative in this study and results in contraction in the strain, which reduces the tensile remaining strain and may eventually increase the compression remaining strain (**Fig. 2**). Therefore the hydraulic pressure decreasing in the above test means a change from self-compression effect dominant to water flow dominant in the model, thus the two effects should be combined together to describe the observed phenomenon.

2.2 Proposed hydraulic pressure model

If the specimen is not fully saturated, the empty voids have the potential to hold the increased volume. Usually the water saturated specimens without special treatment (like vacuum saturation) are not really fully-saturated (95.8% in our test). Therefore, even for the closed test with the non-air entrained samples, there is still enough space to allow the volume increase when ice forms. But since the permeability of cement paste is extremely low, the water flow cannot be fast enough to avoid the hydraulic pressure.

Actually Powers' model was aiming for the hydraulic pressure in the air-entrained cement pastes, which is slightly different with our case (non-air-entrained concrete with different saturation degree). However, the concept and method can be used for this study. Even the air-entrainment agent was not used, the central sphere can still represent the empty space (**Fig. 1**), while the outer influential volume shows the range of pore water that will flow into this empty space. In addition, it is assumed that the liquid water will always occupy the smallest pore first, so if the central sphere represents the empty part, then the surrounding shell should be fully saturated.

If the saturation degree is S_r, the critical radius r_0 between empty and fulfilled pores can be determined by **Fig. 3**, and the pore size distribution can be obtained by experiments or empirical equations (Gong *et al*., 2014). Also in **Fig. 3**, it is assumed that the pores whose radii are bigger than r_0 will stay empty. Here the equivalent radius r_E can be chosen by the weighted mean value of empty volume:

$$r_E = \frac{\int_{\infty}^{r_0} r \cdot v(r) dr}{\int_{\infty}^{r_0} v(r) dr} \tag{3}$$

where $v(r)$ is the volume density of pores. The volume ratio of the central sphere to outer sphere should be equal to the real volume fraction of empty space to the whole material:

$$\frac{r_E^{\,3}}{R_E^{\,3}} = (1 - S_r) \cdot \phi \tag{4}$$

where R_E is the influential volume corresponding to r_E. Using Q to represent the water flow driven by the average pore pressure (p_h) in the surround area, which is:

$$Q = \frac{A}{V} \int q dt \quad \left(A = 4\pi r_E^{\,2}, V = \frac{4}{3}\pi (R_E^{\,3} - r_E^{\,3}) \right) \tag{5}$$

$$q = \frac{k}{\eta} \cdot \frac{\Delta p_h}{\Delta x} \quad \left(\Delta p_h = p_h, \Delta x = (R_E - r_E)/2 \right) \tag{6}$$

The pore pressure (p_h) can be converted to the hydraulic stress (P_H) by the poromechanics, which is:

$$P_H = b p_h \tag{7}$$

where b is the Biot coefficient, and defined as $b = 2\phi/(1+\phi)$ (Coussy, 2004). At the same time, due to this pressure P_H, the material will expand while the liquid and ice will be compressed, that is:

$$\begin{cases} \varepsilon_p = P_H / K_p \\ \varepsilon_C = -p_h / K_C \\ \varepsilon_L = -p_h / K_L \end{cases} \tag{8}$$

where ε_p ε_C ε_L are the volume strain of the porous body, ice and liquid water, respectively. And here linear behavior is assumed for all these three components for convenience. Usually there is plastic deformation on the material, which will be discussed later, here we just choose the simple poroelastic relation. Then the increased volume by ice forming can be balanced by two parts:

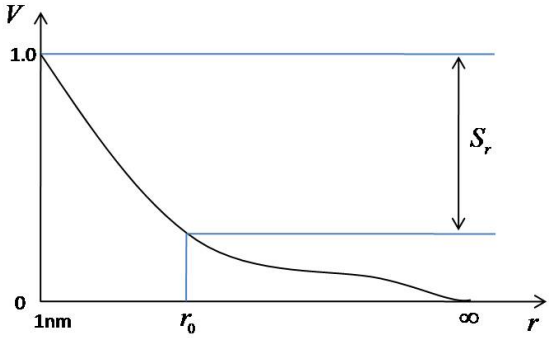

Fig. 3 Typical cumulated pore size distribution.

$$0.09\phi\psi_C - Q = \varepsilon_p - \phi\psi_C\varepsilon_C - \phi\psi_L\varepsilon_L \quad (9)$$

After differentiation of Eq.(9) with respect to time, the following equation is derived:

$$0.09\phi\dot{\psi}_C - \frac{A}{V}\cdot q = \dot{\varepsilon}_p - \phi\psi_C\dot{\varepsilon}_C - \phi\psi_L\dot{\varepsilon}_L \quad (10)$$

Taking Eqs. (5), (6) (7) and (8) into Eq. (10):

$$0.09\phi\dot{\psi}_C - \frac{A}{V}\cdot\frac{k}{\eta}\cdot\frac{2}{R_E - r_E}p_h = \left(\frac{b}{K_p} + \frac{\phi\psi_C}{K_C} + \frac{\phi\psi_L}{K_L}\right)\cdot\dot{p}_h \quad (11)$$

Eq. (11) is the proposed hydraulic model in this paper, if knowing the environmental conditions, moisture conditions and the material properties, the time dependent hydraulic pressure (p_h) can be calculated by solving Eq. (11).

For convenience, let $C_1 = \frac{A}{V}\cdot\frac{k}{\eta}\cdot\frac{2}{R_E - r_E}$, $C_2 = \left(\frac{b}{K_p} + \frac{\phi\psi_C}{K_C} + \frac{\phi\psi_L}{K_L}\right)$ and $C_3 = 0.09\phi\dot{\psi}_C$, then Eq. (11) becomes:

$$C_1\cdot p_h + C_2\cdot\dot{p}_h = C_3 \quad (12)$$

According to Eq. (12) and **Fig. 4**, some basic characters of the modified model can be seen as below:

(1) During the freezing process, ice forms so that $\dot{\psi}_C > 0$, and only part of the increased volume will flow away based on Darcy's law ($C_1\cdot p_h < 0.09\phi\dot{\psi}_C$). Therefore, the hydraulic pressure is increasing according to Eq. (12) ($\dot{p}_h > 0$).

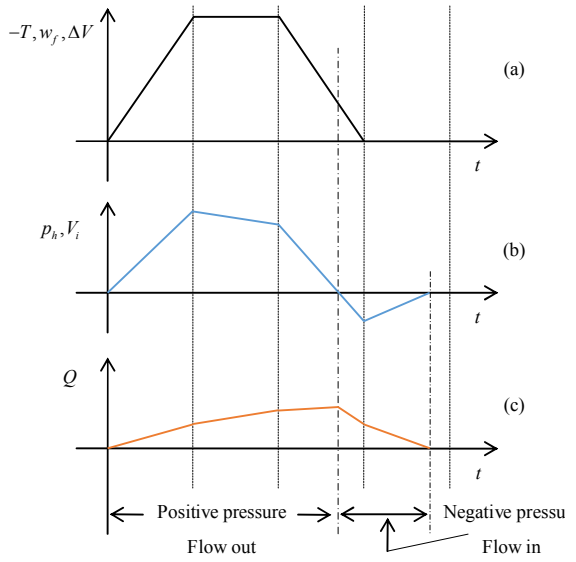

Fig. 4 Change of each parameters (a) temperature (-*T*), frozen water amount (w_f), total increased volume (ΔV) (b) hydraulic pressure (p_h), volume balanced by deformation ($V_i = \Delta V - Q$) (c) the released flow (Q).

(2) When the temperature reaches the lowest value and keeps constant, the ice formation stops ($\dot{\psi}_C = 0$) and C_1 and C_2 are positive, which means p_h and $\dot{p}_h$ should have opposite sign. Since $p_h > 0$, so $\dot{p}_h < 0$, then the hydraulic pressure should still be positive but gradually release.

(3) When the temperature raises up, the ice content will decrease ($\dot{\psi}_C < 0$), the hydraulic pressure will continue to decrease but much faster compared to the constant temperature period. Once the hydraulic pressure becomes negative, the expelled water will move back again from the central void. So it is possible to have short period with negative hydraulic pressure (**Fig. 4 (b)**). At last, all the expelled water during ice formation will move back so the moisture distribution is assumed same as the beginning.

(4) According to different saturation conditions, Eq. (12) can be changed back to Coussy and Monteiro's model or Powers' model. For example, if the release of hydraulic pressure is quite limited ($C_1 \approx 0$, like very high saturation condition), then it becomes: $0.09\phi\psi_C = \left(\frac{b}{K_p} + \frac{\phi\psi_C}{K_C} + \frac{\phi\psi_L}{K_L}\right)\cdot p_h$ which is similar to Coussy and Monteiro's model. If the permeability is higher (like due to frost damage accumulation) so that the water corresponding to increased volume can move to the central void more quickly ($C_2 \approx 0$), then it becomes Powers' model.

2.3 Ice formation and permeability

For porous materials, the freezing point (*T*) of liquid water depends on the curvature of crystal/liquid interface, which is (Scherer, 2005):

$$\kappa_{CL}\gamma_{CL} = \Delta S_{fv}(T_0 - T) \quad (13)$$

where κ_{CL} is the curvature of crystal/liquid interface, γ_{CL} is the specific energy of the crystal/liquid interface. $\Delta S_{fv} \approx 1.2\text{J/cm}^3\cdot\text{K}$ is the molar entropy of fusion. T_0 is the freezing point of free water, here the pure water is assumed for convenience so that $T_0 = 0\,^{\circ}\text{C}$. The curvature κ_{CL} can be also written as:

$$\kappa_{CL} = \frac{2\cos\theta_{CL}}{r - \delta} \quad (14)$$

where θ_{CL} is the contact angle of the crystal/liquid interface, and which can be assumed as 0. *r* is the radius of the pore entry, and δ is the thickness of the liquid film between ice crystal and the pore wall ($\approx 0.9\text{nm}$). Given a certain temperature *T* (*T*<0), it is assumed here that all the pores that are bigger than *r* calculated above would freeze, while the rest would stay unfrozen. Therefore, the ice content (the volume fraction of pore space filled with ice) can be drawn as a function of temperature. There are limited ways to measure the ice content inside the con-

crete, such as the thermoporometry (Sun and Scherer, 2010a; Johannesson, 2010) and electronic method (Cai and Liu, 1998). Among those experimental data, Sun's test (2010a) is chosen to give general characters of ice forming and melting process, because the experiments were more precisely controlled and the results can correlate different variables reasonably and comprehensively, such as the ice content, pore shape, pore size distribution and deformation. In addition, the majority of formed ice is in the smaller pores (r < 100 nm), of which the normalized pore size distributions are very similar among different W/C ratios (Gong *et al*., 2014). Therefore, the ice content of fully saturated specimen can be empirically regressed based on Sun's DSC data (2010a), in regarding with the temperature:

$$w_f = -3.585\times10^{-4}T^2 - 0.0236T \quad (-40^{\circ}\mathrm{C}<T<0^{\circ}\mathrm{C}) \tag{15}$$

$$w_m = \frac{0.449T}{T-2.525} \quad (-40^{\circ}\mathrm{C}<T<0^{\circ}\mathrm{C}) \tag{16}$$

where w_f and w_m are the volume fraction of total voids that occupied by ice during freezing and melting for in a fully saturated case, respectively. The freezing curve (Eq. (15)) and melting curve (Eq. (16)) are not the same, because the freezing point is usually controlled by the size of pore entry while the melting point is by that of pore body (Sun, 2010b), and the pore shape factor λ can be defined as:

$$\lambda = \frac{\Delta T_M}{\Delta T_F} \tag{17}$$

where ΔT_M and ΔT_F is the drop of melting point and freezing point with the same ice content. For the same amount of ice content, ΔT_M is always smaller than ΔT_F. Sun's experimental data show that λ is usually between 0.1 and 0.5 for cement-based materials (Sun, 2010b).

The melting point is always higher than the freezing point for the same pores. If the temperature reaches the lowest value $T_{\min}$, and then increases again, the existing ice would not start to melt immediately, until the temperature reaches $\lambda T_{\min}$ (**Fig. 5**). Thus, the melting curve should be adjusted according to the lowest temperature as:

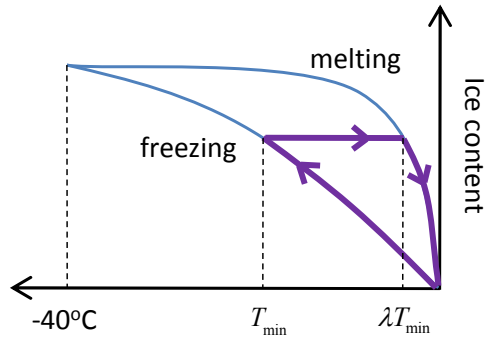

Fig. 5 Freezing and melting curve used in the analysis.

$$w_m = \begin{cases} -3.585\times10^{-4}T_{\min}^{\ 2} - 0.0236T_{\min} & (T_{\min} < T < \lambda T_{\min}) \\ \dfrac{0.449T}{T-2.525} & (\lambda T_{\min} < T < 0^{\circ}\mathrm{C}) \end{cases} \tag{18}$$

If the specimen is partially saturated (S_r<1), which means the biggest pores with volume fraction of (1-S_r) are empty, then the real ice content can be assumed as the value calculated by Eqs. (15) and (16) but subtracted by (1-S_r):

$$\psi_C = \begin{cases} w_f - (1-S_r) & (\text{freezing}, w_f > (1-S_r)) \\ w_m - (1-S_r) & (\text{melting}, w_m > (1-S_r)) \end{cases} \tag{19}$$

The permeability of unsaturated porous material has been well described by the van Genuchten equations as (van Genuchten, 1980):

$$k_r = \frac{k}{k_0} = S_L^{\,0.5}[1-(1-S_L^{\frac{1}{m}})^m]^2 \tag{20}$$

$$S_L = [1+(\frac{P}{P_0})^{1/(1-m)}]^{-m} \tag{21}$$

where k_0 is the permeability of fully saturated material, k is the permeability under the saturation degree of Sr, kr is the relative value that shows the reduction effect. m is the parameter that needs to be determined using Eq. (21), in which the S_r can be experimentally measured as a function of capillary pressure P/P_0. Although van Genuchten equations are originally for soil media and also for the vapor-liquid system, Coussy (2005) has discussed the feasibility to use those equations to describe the cement-based materials and also the effect of ice formation. It has been discussed that the permeability mainly depends on the "liquid saturation", which means no matter the larger pores are occupied by gas or ice crystal or both, they have the same effect on the permeability of liquid water. A more practical expression for cement-based material was given by Coussy (2005) as:

$$S_L = [1+(\frac{R_*}{R_f})^{1/(1-m)}]^{-m} \tag{22}$$

where R_f is the critical pore size for freezing under different temperatures. $R_* = 4.26\text{nm}$ for cement-based materials, which is a factor reflecting the radius of pores which can be percolated to each other. Then the parameter m can be determined according to Sun's DSC data (2010b), and it is approximately equal to 0.5. Therefore, the relative permeability by liquid saturation should be (also see **Fig. 6**):

$$k_r = \frac{k}{k_0} = S_L^{\,0.5}[1-(1-S_L^{\,2})^{0.5}]^2 \tag{23}$$

2.4 Crystallization pressure and cryosuction pressure

Due to the surface tension, there is a pressure difference

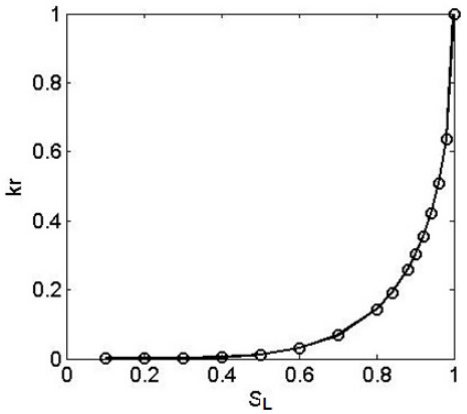

Fig. 6 Relative permeability to liquid saturation degree.

between liquid and crystal on the crystal/liquid interface, and also a difference between liquid and gas on the liquid/vapor interface. If assuming that the pressure of the gas is the same as the ambient pressure (zero), then the cryosuction pressure is always negative, depending on the liquid saturation degree. The pressure uniformity of liquid phase requires that the surface tension of crystal/liquid interface and liquid/vapor interface should be equal:

$$\kappa_{CL}\gamma_{CL} = \kappa_{LV}\gamma_{LV} \tag{24}$$

where κ_{LV} and γ_{LV} represent the curvature and surface energy of liquid/vapor interface respectively. Then, the cryosuction pressure can be related to the freezing point by:

$$\Delta p = -\kappa_{LV}\gamma_{LV} = \Delta S_{fv}(T - T_0) \tag{25}$$

Therefore, the cryosuction pressure can be calculated simply from the temperature distribution:

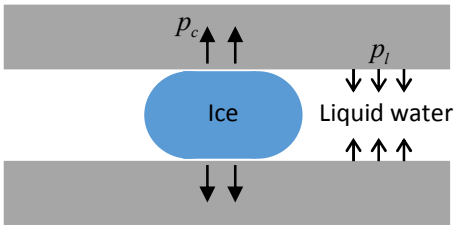

Fig. 7 Crystallization pressure and cryosuction pressure in a cylindrical pore.

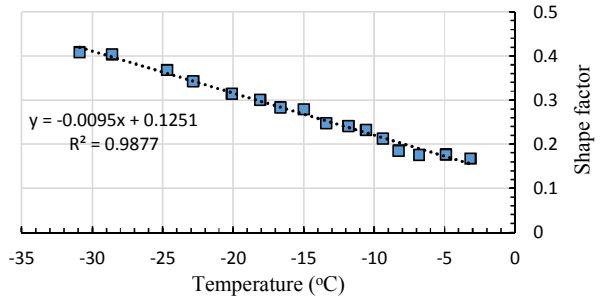

Fig. 8 Pore shape factor as a function of freezing point, based on Sun (2010a).

$$p_l = \psi_L \cdot \Delta S_{fv}(T - T_0) \tag{26}$$

And the crystallization pressure acting on the pore wall is always accompanied with the cryosuction pressure (**Fig. 7**), and also depends on the shape of the pores (λ) based on data from Sun (2010a):

$$p_c = \psi_C \cdot (1-\lambda)\Delta S_{fv}(T - T_0) \tag{27}$$

According to the experimental data (Sun, 2010), the shape factor that defined by Eq. (17) can be approximately rewritten as a linear function of freezing point (**Fig. 8**), then, Eq. (27) becomes:

$$p_c = \psi_C \cdot (0.875 + 0.0095T)\Delta S_{fv}(T - T_0) \tag{28}$$

3. Comparison to test results

3.1 Experiment and simulation

The mortar specimens in this experiment (Sicat *et al.* 2013) used ordinary Portland cement with density of 3.14 g/cm^3, fine aggregate which is 1.2mm or less in size with density of 2.67 g/cm^3 at 1467.6 kg/m^3 of concrete without air entraining agent to promote damage. Mix proportion for specimens is 1:2:6 (water: cement: fine aggregate). After curing, specimens were cut into size of 40mm x 40mm x 2mm (see **Fig. 9 (a)**). Specimens were submerged underwater until mass was constant to attain full saturation. Finally, the specimens were sealed with vinyl tape to prevent water uptake or loss. The preparation of the specimens is shown in **Fig. 9 (a)** and **(b)**. The size distribution of entrapped air can be obtained from image anlysis (**Fig. 9 (c)**). The critcal radius r_0 between empty and fullfilled pores can be estimated combining pore size information and saturation condition (Gong *et al.* 2014), which is shown in **Table 1**.

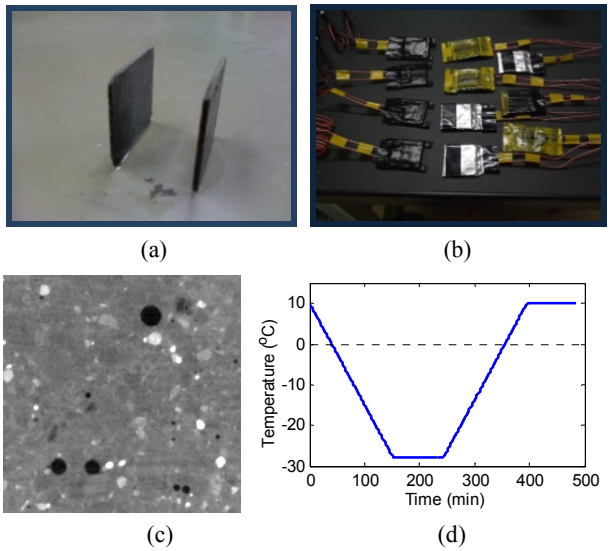

Fig. 9 Outline of the experiment (a) 40 x 40 x 2mm cut specimens; (b) sealed specimens; (c) X-ray CT scanning (6.2x6.2mm).

Table 1 Parameters by experimental measurements.

Type (w/c)	Mortar (0.5)
Mix proportion by weight (water: cement: aggregate)	1:2:6
Water saturated (vacuum saturated)	0.228 g/cc (0.238g/cc)
Real water saturation (compared with vacuum saturation)	0.958
Critical radius r_0 (by X-ray CT scanning)	1.7×10^{-4}m
Lowest temperature	-28°C
Cooling rate (also heating)	15 °C/h
Elastic modulus of concrete material E (measured)	34 GPa

Table 2 Parameters by empirical estimation.

Saturated permeability (undamaged) k_0	10^{-21}m^2
Viscosity of water η (Coussy, 2005)	2.88×10^{-5} exp[509.53 /(123.15+T)] Pa·s
Poisson's ratio of concrete material v	0.2
Bulk modulus of porous body $K_p = E/[3(1-2v)]$	18.9 GPa
Bulk modulus of ice crystal K_C	8.8 GPa
Bulk modulus of liquid water K_L	2.2 GPa
Critical radius r_0 (by empirical equations)	2×10^{-4}m
Equivalent r_E (by Eq. (3))	6×10^{-4}m
Equivalent R_E (by Eq. (4))	0.0028m

Finally **Fig. 9 (d)** shows the temperature history of each cycle.

Reasonable parameters are chosen for the calculation model (see **Table 2**). The critical radius (r_0, the radius between empty pores and pores filled with water according to **Fig. 3**) can also be estimated using the empirical pore size distribution (Gong *et al*. 2014), and for the macro pores (r>10μm), the estimation formula is (Shimomura *et al*, 1992):

$$v(r) = V(\infty)\cdot B\cdot C\cdot r^{C-1}\cdot\exp(-B\cdot r^{C}) \tag{29}$$

where $v(r)$ is the density of pore volume of concrete or mortar, $V(\infty)$ is the total pore volume of unit concrete, r is the radius of pore (m), B and C are the parameters depending on the water cement ratio w/c. If w/c=0.5, the empirical values were given as $V(\infty)=0.015$, B=12000, and C=1.2 (Takewaka *et al*, 2003). The estimated r_0 is 2×10^{-4}m, which is quite close to the value calculated based on the information in Sicat *et al*.'s paper (2013), which is 1.7×10^{-4}m. Therefore, the empirical estimation is reliable and easier to be applied to other cases.

Adopting the parameters listed in **Table 1** and **Table 2** to the proposed model, the three kinds of pore pressure can be calculated (**Fig. 10**). The crystallization and cryosuction pressures are always coexisted and the sum of two pressures are always less than or equal to zero.

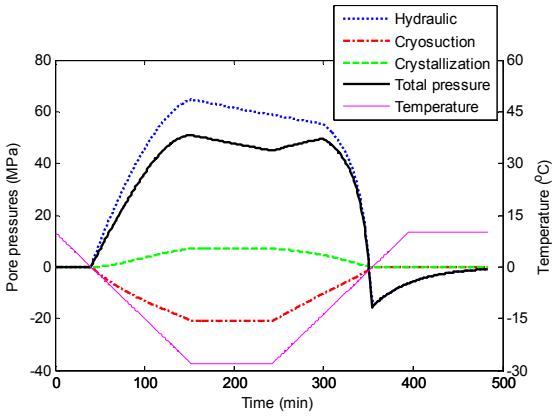

Fig. 10 Simulated hydraulic, crystallization and cryosuction pressures.

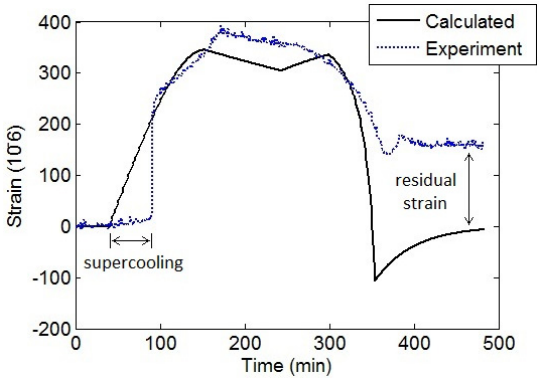

Fig. 11 Calculated strain and experimental test (first cycle, $k_0 = 10^{-21}$ m^2).

The hydraulic pressure is closely related to the permeability (k_0), for the first freeze/thaw cycle, the permeability of undamaged material can be assumed, which is around 10^{-21}m^2 according to Valenza and Scherer's beam-bending test (2004). Thus, for closed test without water uptake, the hydraulic pressure will reach the maximum value during first FTC, and then reduce gradually. The total pressure (sum of three pressures in **Fig. 10**) is still positive, which means expansion occurs at the beginning. In **Fig. 10**, the crystallization pressure and cryosuction pressure are calculated by Eq. (28) and Eq. (26). The hydraulic pressure is calculated by Eq. (11). The basic characters of hydraulic pressure in **Fig. 10** is in agreement with the discussion of **Fig. 4**.

It is difficult to measure the pore pressure in cementitious materials directly, however, the measured strain can be used to verify the model sufficiently, because the total deformation directly results from the total internal forces. More precisely, the stress-strain relationship of the porous body is nonlinear under the high pressure condition, and the plastic deformation was also observed during the experiment as seen in **Fig. 11**. The detailed stress-strain relation under cyclic freeze thaw has been discussed in previous work (Gong *et al*. 2013). The plastic deformation is mainly shown as the residual strain, but for the peak strain of each cycle, it is still almost linear to the stress level. Therefore, in order to focus on the hydraulic

model proposed in this study, a simple stress-strain relation is assumed. Then according to the poroelastic theory, the one-dimensional strain should be:

$$\varepsilon_x = \left(\frac{b}{3K_p}\right)\left(p_h + p_l + p_c\right) \tag{30}$$

From **Fig. 11**, it can be seen that the estimated strain matches experimental measurements well. The difference between the nucleation temperatures is because the nucleating agent (metaldehyde) was used in Sun's test (where we took the ice amount information from). While in our test, the super cooling effect existed because nucleating agent was not used. Although the freezing point of bulk water should be at 0°C, if the water is too pure and lack of nucleating particles, the freezing point can still drop below 0°C, such as -8°C in our test. However, this difference does not affect the stress level as temperature continues to decrease. Another difference in **Fig. 11** is the residual strain resulting from the plastic deformation, which is just a response of the material and thus ignored in this model. Here it should be emphasized that the main purpose of this work is to develop the stress model which can express both the self-compaction self-compression effect and pressure release effect, further to describe the deformation tendency in closed condition for moisture. In order to make the model simple, the stress model is still based on poroelastic theories, although plastic deformation actually exists during the test. And also, since the strain is usually within a few hundreds of microns, there is no big difference between stress estimated by elastic model and plastic model. If only concerning the plastic deformation as a "response" of the material, this materials property can be discussed separately, like author's previous work (Gong, *et al.* 2013). Therefore, the influence of the plastic behavior is not taken into consideration in this model.

3.2 Reduction of hydraulic pressure

As discussed at the beginning, once the moisture content is constant, the crystallization pressure and cryosuction pressure only depend on the pore size distribution of micro pores(r<100nm), which has been observed unchanged within 3 cycles in Sun's test (2010b). Thus, these two kinds of pressures can be assumed unchanged in the following cycles. Then we only need to focus on the hydraulic pressure. From Eq. (11), the three most important factors are cooling rate, saturation degree and permeability. Cooling rate is set manually and kept constant during the test. The change of saturation degree can be also neglected (even a residual strain of 500μ is corresponding to 0.1% volume increase of empty space). Therefore, the reduction of hydraulic pressure mainly results from the change of permeability. Actually previous studies also observed permeability increase by frost damage (Yang *et al.* 2006). This increment of permeability or reduction of hydraulic pressure is mainly due to the occurrence of micro cracks during the early freeze-thaw cycles, which might change the micro structure in mortar although the pore size distribution might still be unchanged. Thus, the hydraulic pressure would be continuously reduced in the latter cycles.

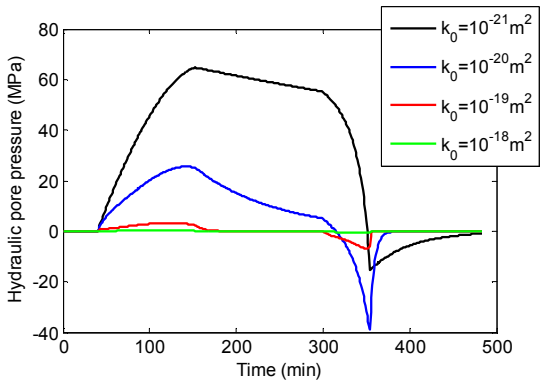

Fig. 12 Calculated hydraulic pore pressure with different permeability.

Then by increasing the permeability, the reduction of hydraulic pore pressure can be calculated (**Fig. 12**). It should be noticed that in reality, negative hydraulic pressure cannot reach -40MPa, because liquid water has good capability for compression but not tension. Still here, in order to reduce the complexity of the model, this aspect is not considered.

Figure 13 shows the comparison between estimated strain and measured strain. The 4th and 28th cycle are

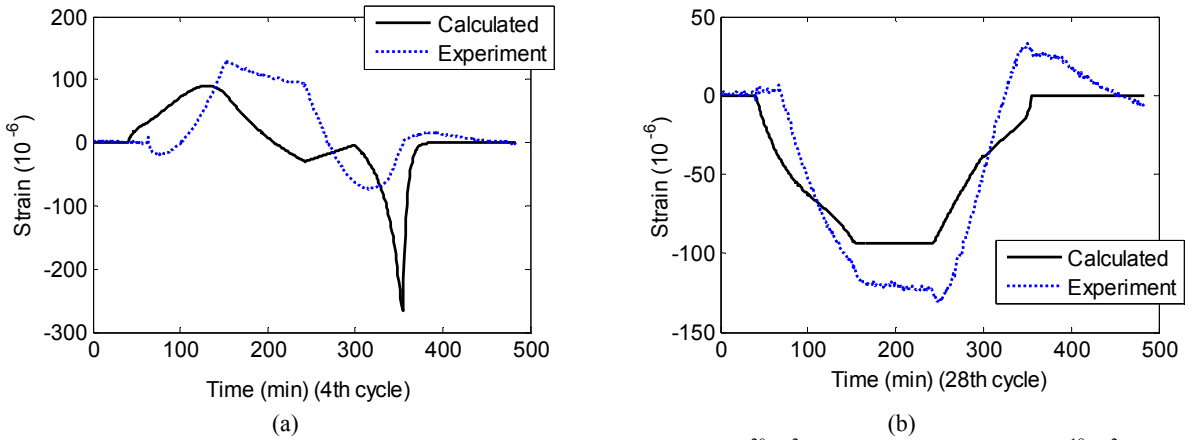

(a) (b)

Fig. 13 Calculated and experimental strain (a) 4th cycle, $k_0 = 10^{-20}\,\mathrm{m}^2$ (b) 28th cycle, $k_0 = 10^{-18}\,\mathrm{m}^2$.

chosen to show the typical change of the strain behavior, which are corresponding to the permeability of $10^{-20}m^2$ and $10^{-18}m^2$, respectively. Although it is difficult to measure the permeability during the test, the above values of permeability can be estimated based on the following arguments: first it is proved that the permeability change is the reason of the reverse phenomenon in the test, and it is also qualitatively known that the permeability will increase due to frost damage (Yang *et al*. 2006). Therefore a proper value of permeability should be existed that can match the observed behavior best. Together with **Fig. 11**, three kinds of typical strain behavior are shown: State 1: always expansion dominant; State 2: change from expansion to contraction; and State 3: always contraction dominant. Actually State 2 is a transition state between State 1 and 3, and State 3 is a final steady state in the closed test.

4. Discussions

According to the comparison and discussion above, the reliability of the proposed model can be verified, then deeper discussions are able to be made. The most affective parameters are cooling rate, saturation degree and the permeability. Among three factors, the cooling rate is certain and controlled manually; the saturation degree is considered constant in closed test, but it will increase in the open test. Finally, the change of permeability is due to the damage caused by hydraulic pressure, and at the same time, the hydraulic pressure will decrease if permeability becomes larger, so an equilibrium steady state can be achieved at last.

Setting the cooling rate as 15°C/h, the hydraulic pore pressure (maximum value) can be obtained regarding the vacuum saturation degree, and for each level of permeability (**Fig. 14**). It is certain that the peak pressure would decrease as saturation degree decreases, and also as permeability increases. The effect of permeability becomes less significant if S_r is closed to 100%. It is because once all the empty spaces are filled up, the water flow and pressure release will stop so that the permeability has no effect on the stress. Therefore, in the closed test, we can observe a big changing tendency from expansion to contraction due to the permeability change. But in the open test, the saturation degree will increase gradually due to the water uptake. For example, if S_r=99%, the permeability change would not reduce the hydraulic pressure effectively, then there is always expansion in the open test. It is also easy to understand that higher cooling rate will result in higher hydraulic pressure, as shown in **Fig. 15**. And for the 95.8% saturation, the permeability has a great effect on the calcualted pressure.

The permeability is a very important factor for concrete durability. Previous study only discussed the permeability increase qualitatively (Yang *et al*. 2006) and indirectly (by testing the water absorption speed). However, there are only few direct experimental measurements on it. One reason is that the damage is difficult to evaluate under different frost conditions. And also the permeability itself is not easy to be measured for concrete materials. Here the proposed model can provide a "back analysis" way to evaluate the permeability change. For example, **Fig. 16** shows peak value of the hydraulic pore pressure depending on permeability, which will decrease if the permeability increases due to damage. Then once the magnitude of hydraulic pressure can be estimated according to the measured deformation, it is

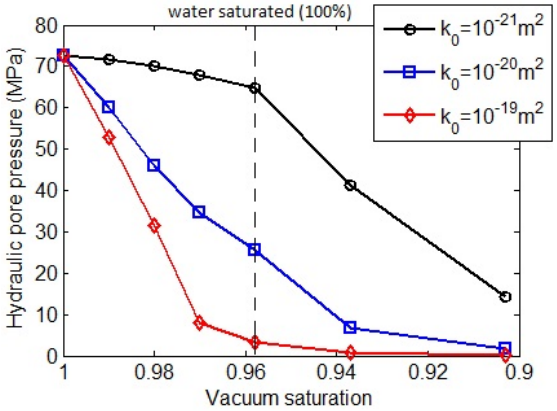

Fig. 14 Hydraulic pore pressure (peak value) change with vacuum saturation degree (cooling rate=15°C/h).

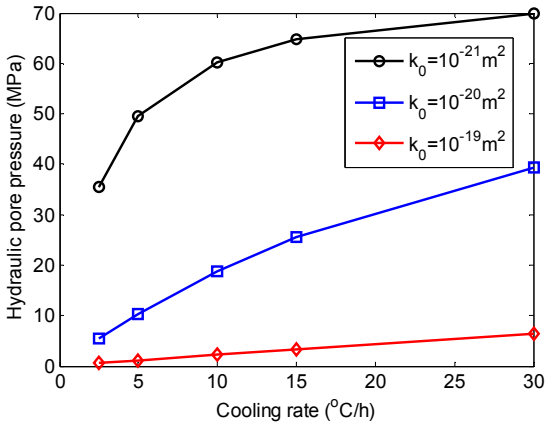

Fig. 15 Hydraulic pore pressure change with cooling rate (S_r=95.8%).

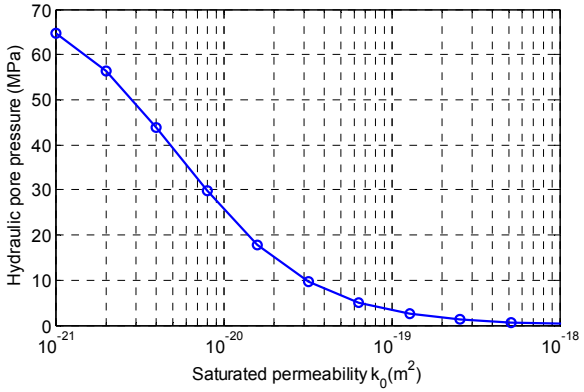

Fig. 16 Hydraulic pore pressure reduction as permeability increases (cooling rate=15°C/h, S_r=95.8%).

also possible to calculate the change of permeability accordingly. Considering the fact that the permeability of concrete materials are usually difficult to measure, and also the permeability increment by frost damage is also a crucial problem for concrete durability, it is much more convenient to apply this model to predict the permeability change by frost damage. The model does not need additional test and can be applied to any environmental conditions. However, if making this model to a testing method, more experimental verifications are needed, which will be conducted in the future studies.

5. Conclusions

In this paper, a comprehensive hydraulic pressure model is proposed, trying to cover all the existing main mechanisms. The poromechanical rules and Darcy's law are combined to calculate the hydraulic pressure, which becomes a half static and half dynamic force. The hydraulic pressure is closely depending on the permeability of the material, and might decrease gradually at the number of freeze thaw cycles increases. The total pressure is the combination of three pressures (hydraulic, crystallization and cryosuction), which will be positive at the beginning but convert to be negative later. This mechanism explains the reverse phenomenon of the strain during test with closed moisture condition.

The experimental measurements are used to verify the reliability of the proposed model. Poroelastic relation is assumed to estimate the strain based on the calculated total pressure, and the estimated strain is in good agreement with experiment data.

The effect of the main parameters on the calculated results is also discussed. The saturation degree plays a crucial role in the super high saturation region (higher than 96%), which makes the reverse phenomenon only happens in test with closed moisture condition but not in open condition. And at last, the permeability change is a result of frost damage, but at the same time, the increased permeability will help to reduce the stress level, and finally the system will achieve an equilibrium steady state.

The relationship between stress level and permeability revealed by this model can also provide a possible way to evaluate the durability problem under a given environmental condition. That is, after a certain number of freeze thaw cycles, we can estimate the permeability according to the strain behavior during that cycle. This quick method is convenient, based on the same specimen, and the permeability can be tracked during the entire test. But the reliability needs further investigation (for example, by comparing with direct permeability measurements), which will be conducted in the further work.

Acknowledgements

The authors would like to express their sincere thanks to Japan Society for the Promotion of Science (JSPS) for providing the fellowship to the Doctor's study and also the Grant-in-Aid for Scientific Research (A) No. 26249064.

References

Coussy, O., (2004), "*Poromechanics*." Wiley, West Sussex, England.

Coussy, O., (2005), "Poromechanics of freezing materials." *Journal of the Mechanics and Physics of Solids*, 53, 1689-1718.

Coussy, O. and Monteiro, P. J. M., (2008), "Poroelastic model for concrete exposed to freezing temperatures." *Cement and Concrete Research*, 38, 40-48.

Coussy, O. and Monteiro, P. J. M., (2009), "Errata to "Poroelastic model for concrete exposed to freezing temperatures" [Cement and Concrete Research 38 40-48]", *Cement and Concrete Research*, 39, 371-372.

Fagerlund, G., (2002). "Mechanical damage and fatigue effects associated with freeze-thaw of materials." *Proceedings of International RILEM Workshop of Frost Resistance of Concrete*, April 2002, 117-132.

Gong, F., Sicat, E., Ueda, T. and Zhang, D., (2013), "Meso-scale mechanical model for mortar deformation under freeze thaw cycles." *Journal of Advanced Concrete Technology*, 11, 49-60.

Gong, F., Zhang, D., Sicat, E. and Ueda, T., (2014), "Empirical estimation of pore size distribution in cement, mortar and concrete." *Journal of Materials in Civil Engineering*, 26(7), 04014023-1-11

Hasan, M., Okuyama, H., Sato, Y. and Ueda, T., (2004). "Stress-stain model of concrete damaged by freezing and thawing cycles." *Journal of Advanced Concrete Technology*, 2(1), 89-99.

Johannesson, B., (2010). "Dimensional and ice content changes of hardened concrete at different freezing and thawing temperatures." *Cement and Concrete Composite*, 32, 73-83.

Kaufman, J. P., (2002). "A qualitative sequential frost deicing salt damage model based on experimental data." *Proceedings of International RILEM Workshop of Frost Resistance of Concrete*, April 2002, 197-204.

Power, T. C., (1949), "The air requirement of frost-resistant concrete." *Proc. Highway Res. Board*, 29, 184-211.

Scherer, G. W. and Valenza II, J. J., (2005). "Mechanism of frost damage." In: Skalny, J. and Young, F. Eds. *Materials Science of Concrete Vol. VII*: American Ceramic Society

Shimomura, T. and Ozawa, K., (1992). "Analysis of water movement in concrete based on micro pore structure model." Proceedings of JCI, 14(1), 631-636. (Japanese)

Sicat, E., Gong, F., Zhang, D. and Ueda, T., (2013). "Change of the coefficient of thermal expansion of mortar due to damage by freeze thaw cycles." *Journal of Advanced Concrete Technology*, 11, 333-346.

Sun, Z. and Scherer, G. W., (2010a), "Effect of air voids on salt scaling and internal freezing." *Cement and Concrete Research*, 40, 260-270.

Sun, Z. and Scherer, G. W., (2010b), "Pore size and shape in mortar by thermoporometry." *Cement and Concrete Research*, 40, 740-751.

Takewaka, K., Yamaguchi, T. and Maeda, S., (2003), "Simulation model for deterioration of concrete structures due to chloride attack." *Journal of Advanced Concrete Technology*, 1, 139-146.

Valenza II, J. J. and Scherer, G. W., (2004), "Measuring permeability of rigid materials by a beam-bending method: V, Isotropic rectangular plates of cement paste." *J. Am. Ceram. Soc.*, 87 (10),1927-1931.

Van Genuchten, M. Th., (1980). "A closed-form equation for predicting the hydraulic conductivity of unsaturated soils." *Soil Sci. Soc. Am. J.*, 44, 892-898.

Yang, Z., Weiss, W. J. and Olek, J. (2006), "Water transport in concrete damaged by tensile loading and freeze-thaw cycling." *Journal of Materials in Civil Engineering*, 18(3), 424-434.

Notations

E — Elastic modulus of porous body (GPa)
v — Poisson's ratio of material
K_p — Bulk modulus of porous body (GPa)
K_C — Bulk modulus of ice crystal (GPa)
K_L — Bulk modulus of liquid water (GPa)
k — Actual permeability (m^2, $k = k_0 \cdot k_r$)
k_0 — Saturated permeability (m^2)
k_r — Relative factor of permeability
η — Viscosity of liquid water ($Pa \cdot s$)
K_{CL} — Curvature of liquid/crystal interface
κ_{LV} — Curvature of liquid/vapor interface
γ_{CL} — Specific energy of liquid/crystal interface
γ_{LV} — Specific energy of liquid/vapor interface
ΔS_{fv} — Molar entropy of fusion ($J/cm^3 \cdot K$)
λ — Pore shape factor
ϕ — Void ratio
b — Biot coefficient ($= 2\phi/(1+\phi)$)
ε_p — Volume strain of porous body
ε_C — Volume strain of ice crystal
ε_L — Volume strain of liquid water
ε_x — Strain of porous body in one dimension
w_f — Ice content during freezing (for saturated condition)
w_m — Ice content during melting (for saturated condition)
ψ_C — Ice content (percent of the total void)
ψ_L — Liquid content (percent of the total void)
S_r — Total saturation (ice + liquid)
S_L — Liquid saturation ($=\psi_L$)
S_C — Ice crystal saturation ($=\psi_C$)
p_h — Hydraulic pore pressure (MPa)
p_l — Cryosuction pressure (MPa)
p_c — Crystallization pressure (MPa)
r_0 — Critical radius of empty pores (m)
$v(r)$ — Volume density of pores
r_E — Equivalent radius of empty space (m)
R_E — Radius of influential volume (m) of r_E
A — Surface area of the equivalent empty space ($A = 4\pi r_E^2$)
V — Volume of the influential volume ($V = 4/3 \cdot \pi(R_E^3 - r_E^3)$)
P_H — Hydraulic stress caused in the material (MPa)
q — Flow into and out of empty pores (m/s)
Q — Amount of released liquid water
R_f — Critical radius of freezing temperature
R_* — Parameter reflecting the percolation of pores (= 4.26nm)